COMMUNICATIONS IN NUMERICAL METHODS IN ENGINEERING
Commun. Numer. Meth. Engng, **14**, 849–861 (1998)

A DISCRETE NON-LOCAL (DNL) OUTGOING BOUNDARY CONDITION FOR DIFFRACTION OF SURFACE WAVES

R. P. BONET,* N. NIGRO, M. A. STORTI AND S. R. IDELSOHN
Grupo de Tecnología Mecánica del INTEC, Güemes 3450, 3000 — Santa Fe, Argentina

SUMMARY

A discrete non-local (DNL) boundary condition is used to solve the water waves propagation problem over variable depth. This condition is obtained by means of full solution of the discrete Helmholtz operator in a structured network. We consider a simulation of wave propagation around a circular island located on either a paraboloidal shoal or constant depth bathymetry. Such examples confirm the important improvement in accuracy for the DNL method over standard conditions in the near field. © 1998 John Wiley & Sons, Ltd.

KEY WORDS outgoing boundary condition; Berkhoff; discrete; non-local; surface waves; scattering

1. INTRODUCTION

When a long wave (for example, a tsunami) is propagating over waters of variable depth, it may be greatly amplified due to the variation of sea bed topography and/or at the coast; this is a highly non-linear phenomenon. The scattering of waves by a circular island located on a paraboloidal shoal is a well-known problem of long wave propagation;[1–11] (see Figure 1).

The calculation of diffraction of water waves over a varying sea bed, based on finite element methods, was done by Berkhoff[12] and Chen and Mei[13–15] initially. Chen and Mei used a Fourier–Bessel expansion as an exterior solution in a wave diffraction problem and a specially devised variational statement to link the exterior solution with finite element solutions in the interior domain.

Zienkiewicz *et al.*[6–9] made an important contribution in this way, when they proposed a general methodology for the solution about this problem. There were several strategies which allowed one to link finite element solutions to any kind of Helmholtz equation exterior solution (analytical, series or boundary integral).

This problem has also been solved by Tsay and Liu,[16] Houston,[17] Xu *et al.*[18] and Bonet,[19] who incorporated the exact radiation condition at infinity in the numerical scheme by means of a 'sponge-filters' method.

Different procedures based on 'infinite elements' to solve the exterior problem governed by the Helmholtz equation on an unbounded domain are given by Zienkiewicz and Bettess[10,11] and H. S. Chen.[20] They used of 3- and 2-node shape functions, respectively, to approximate the

* Correspondence to: R. P. Bonet, Grupo de Tecnologia Mecania, INTEC, Guemes 3450, 3000 Santa Fe, Argentina.
E-mail: rbonet@venus.unl.edu.ar

Contract grant sponsor: CONICET, Argentina; BID 802/OC-AR PID 26.
Contract grant sponsor: Universidad Nacional del Litoral, Argentina.

CCC 1069–8299/98/090849–13$17·50

Received 16 September 1997
Accepted 13 February 1998

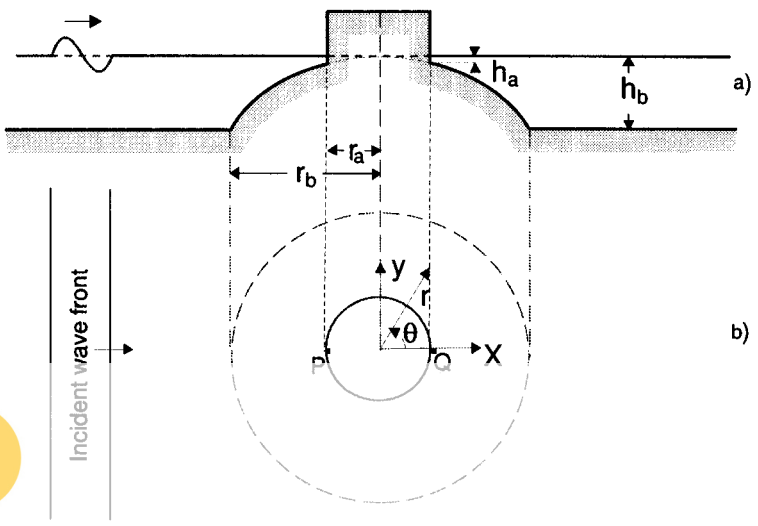

Figure 1. Sketch of the idealized island on a paraboloidal shoal with $h = \alpha r^2$; (a) vertical: $r_a = 10$ km, $r_b = 30$ km, $h_a = 0{\cdot}444$ km, $h_b = 4$ km; (b) horizontal (after Jonsson *et al.*[2]

exterior solution. However, such shape functions are strictly valid only in the far field, in terms of the radial distances r. These procedures have the advantage that the integrals involving the infinite elements can be integrated analytically.

An entirely different procedure to impose the radiation condition at infinity is given by D. Givoli[21,22] by means of the DtN method, which has been developed by Harari[23] for acoustic problems. This boundary condition is exact and non-reflecting, but the base system must be selected according to the space dimension of the problem at hand. It is easily implemented in a finite element method.[23] However, due to the truncated DtN map being non-local in space, the resulting system of linear equations is not sparse.

In contrast with the methods described earlier, a discrete formulation to impose the radiation boundary condition at infinity in a numerical scheme can be developed directly. R. W. Thatcher[24] used an infinite number of triangular elements (defined in a systematic way) for approximating the solution of Laplace's equation in unbounded regions. This method suggests finding the general solution of a recurrence relationship, which involves finding the complete eigensolution of a matrix. When the general solution of the recurrence relationship is given analytically,[25] the method is extremely easy to implement.

Other methods, based on cloning-type algorithms, have been developed by Dasgupta,[26] and Wolf and Song.[27,28] In Reference 28 Wolf and Song describe the consistent infinitesimal finite element cell method to model the unbounded medium for the scalar and vector wave equation of elastodynamics and diffusion in the frequency and time domains. This method is a boundary finite element procedure, which requires the discretization of the artificial boundary only and is exact in the finite element sense. After performing the limit of the infinitesimal cell width, the unbounded domain is thus cloned.

A discrete non-local DNL formulation for a finite element method on an unbounded domain has been developed by Bonet *et al.* recently.[29–31] This formulation is based on the general solution

of a recurrence relationship which involves the complete eigendecomposition of the discretized operator (as well as Thatcher's method[24]) over a structured mesh with quadrangular linear elements. This formulation, like the consistent infinitesimal finite element cell method,[28] requires discretization on the artificial boundary only. The planar DNL boundary condition is non-local in space (as well as the truncated DtN map) and non-reflective.

In this paper we employ a formulation for a bounded computational domain that are derived by the DNL method for the circumferential case. The DNL procedure represents a general methodology. It has been applied to solve exterior problems associated with the Helmholtz operator,[29,31] employing the finite difference (FDM) or finite element (FEM) method, as well, in the solution of the ship wave resistance problem.[32] By means of this procedure the exterior problem associated with the Berkhoff equation[12] is solved numerically, and a DNL boundary condition over the artificial boundary is obtained. This condition has the ability to describe scattered waves in all directions adequately, yet in the near field.

We present the shallow water diffraction solution for the scattering of water waves by a circular island and we compare the cases when the island is and is not located on a paraboloidal shoal. These numerical tests validate the numerical method employed.

2. FORMULATION

We consider the scattering from a bounded region Ω in two-dimensional space. This region is limited by a circumference $\mathcal{B}$ of radius r_i centred at the origin. Outside from the circle limited by $\mathcal{B}$ (denoted Ω') (i.e. outside the shoal) we assume that both the incident wave field $\eta_i(x, y)$ and the scattered wave field $\eta^s(x, y)$ independently satisfy the Helmholtz equation,

$$\Delta\eta + k_0^2\eta = 0 \tag{1}$$

where $k_0 (= 2\pi/\lambda_0)$ is the wave number corresponding to the constant depth.

The scattered wave field η^s satisfies the Sommerfeld radiation condition,[12]

$$\lim_{r\to\infty} \sqrt{(k_0 r)}\left(\frac{\partial}{\partial r} - ik_0\right)\eta = 0 \tag{2}$$

We suppose that the domain Ω within $\mathcal{B}$ is bounded internally by the smooth surface Γ (see Figure 2). In the region with variable water depth (i.e. in the region over the shoal) the time-independent part of the water elevation $\eta(x, y)$ satisfies the long-wave equation[2]

$$\nabla(h\nabla\eta) + k^2 h\eta = 0 \text{ in } \Omega \tag{3}$$

where ∇ is the horizontal gradient operator, ω is the angular frequency, g is the gravitational acceleration, and $h = h(x, y)$ is the water depth. $C = C_g = \sqrt{(gh)}$ are the phase and group velocity, respectively; $k = \omega/C \geqslant 0$ is the wave number, such that $k(x, y)$ changes continuously until to the boundary $\mathcal{B}$, where it takes the value k_0. (This theoretical formulation is classical and you can find it expressed in other papers, of different forms, for example in References 2, 9 and 26.)

In the external region to Ω the numerical solution is derived by means of a partial discretization process. Details are included in the following Sections.

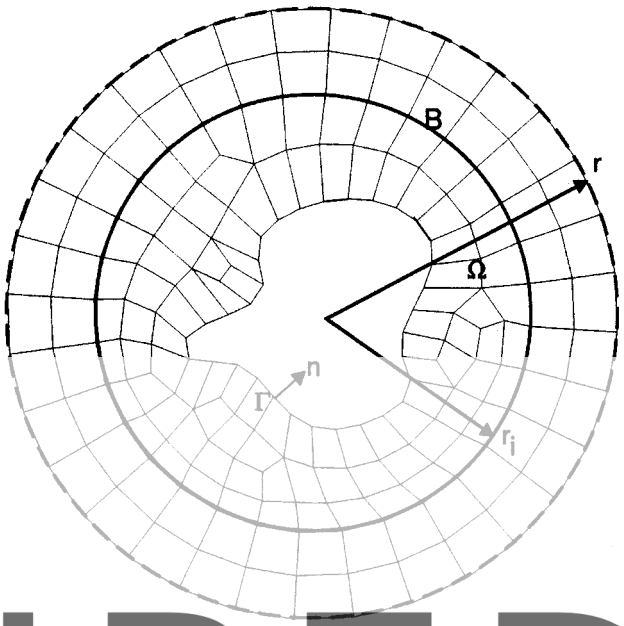

Figure 2. A model domain for radiation and scattering problem

3. THE DNL FORMULATION

The circumferential DNL procedure is based on the full solution of the exterior problem governed by the discretized Helmholtz operator with constant refraction index. For this, the unbounded domain (in the external region to Ω_i (see Figure 2)) is subdivided into two parts—a bounded region (the annular region $r_i \leqslant r \leqslant r_e$, $-\pi \leqslant \theta \leqslant \pi$ (see Figure 3)) and an unbounded semi-infinite region (the region $r \geqslant r_e$). Figure 3 (left) shows the scatterers surrounded by a circle

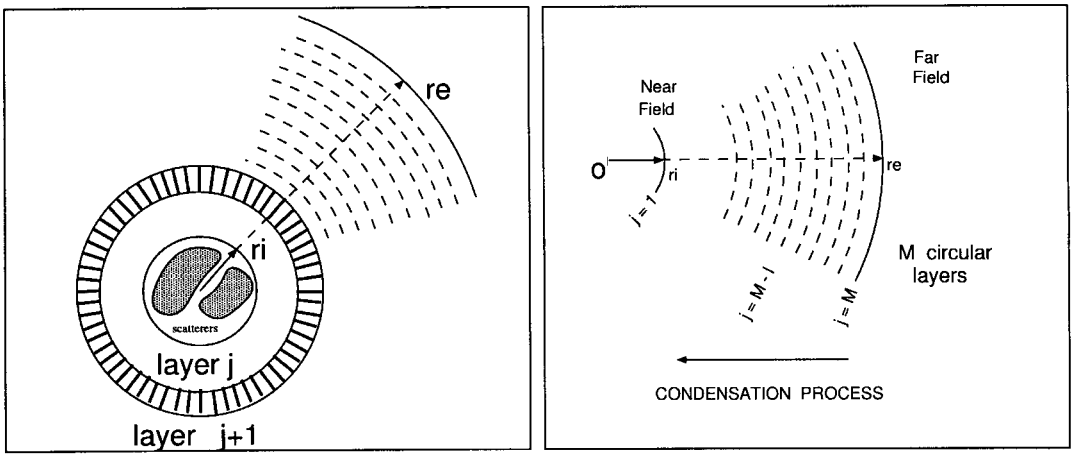

Figure 3. Circular DNL method: (left) sketch on the scattering process by DNL method; (right) condensation process

of radius r_i, located at the artificial boundary (in the near field) and the successive circles (0 layers) until the circle $r = r_e$ (in the far field), which is taken sufficiently large such that the influence of curvature can be neglected. In contrast with Thatcher's method,[24] the DNL method uses a discretization with quadrangular linear elements (see layer j in Figure 3), resulting in extremely easy implementation. The crucial issue is, first, the adequate representation of the scattered wave field in the far field ($r \geqslant r_e$), and second, in the near field (where is located the artificial boundary of the computational domain ($r = r_i$)).

We describe here briefly such a procedure performing the partial discretization of the Helmholtz equation (1) in polar co-ordinates, with quadrangular linear elements. Integrating in the transversal direction θ, we obtain a second order differential equation system in r of the form

$$\mathbf{I}\ddot{\eta} + \frac{1}{r}\mathbf{I}\dot{\eta} - \frac{1}{r^2}\mathbf{M}^{-1}\mathbf{K}\eta + k_0^2\mathbf{I}\eta = \bar{0} \tag{4}$$

where $\eta = \eta^s$, $\dot{\eta} = \mathrm{d}\eta^s/\mathrm{d}r$, $\mathbf{M}$ and $\mathbf{K}$ are the mass and stiffness assembled matrices, respectively, and $\mathbf{I}$ is the identity matrix. Discretization of equation (4) in r can be done by the finite difference method or the finite element method. Independently of the partial discretization procedure employed, the corresponding discrete equation for layer j has the form

$$\mathbf{C}^j\eta^{j-1} + \mathbf{B}^j\eta^j + \mathbf{A}^j\eta^{j+1} = 0 \tag{5}$$

where η^j is the vector containing potential values for the nodes on layer j. We note that, unlike for the rectangular geometry case, here $\mathbf{A}^j$, $\mathbf{B}^j$ and $\mathbf{C}^j$ are different matrices at successive layers, due to the r^j factors.

3.1. DNL method in the far field

To obtain the DNL condition in the near field it is necessary to obtain the DNL condition in the far field, where the curvature effects can be neglected. We denote this layer by $j = M$ (see Figure 3). For layer $j = M$ (5) reduces to

$$\mathbf{A}^M\eta^{M-1} + \mathbf{B}^M\eta^M + \mathbf{A}^M\eta^{M+1} = 0 \tag{6}$$

The $\mathbf{A}^M$ and $\mathbf{B}^M$ matrices are real, and cyclic in virtue of their periodicity. Their dimension is $N_{\mathrm{lay}} \times N_{\mathrm{lay}}$. We consider that the $\mathbf{A}^M$ and $\mathbf{B}^M$ matrices remain almost constant for the layer $j \geqslant M$ (in the semi-infinite region $r \geqslant r_e$), and it allows the application of the planar DNL method.[30] Then, we denote $\mathbf{A}^M = A$ and $\mathbf{B}^M = B$ for the layer $j \geqslant M$.

For the real matrix $A^{-1}B$, there is an orthogonal transformation V, such that

$$A^{-1}B = V\Lambda V^{-1} \tag{7}$$

where $\Lambda = \mathrm{diag}(\lambda_1, \lambda_2, \ldots, \lambda_{N_{\mathrm{lay}}})$ is a diagonal matrix formed by the eigenvalues of the $A^{-1}B$ matrix and V is the eigenvector system of $A^{-1}B$.

By means of the non-singular transformation

$$\eta_l^j = \sum_{i=1}^{N_{\mathrm{lay}}} V_{l,i}(c_i^+\mu_i^{+j} + c_i^-\mu_i^{-j}), \quad l = 1, 2, \ldots, N_{\mathrm{lay}} \tag{8}$$

the scattered wave field is split into 'forward' and 'backward' propagation modes, where $\mu_i^{\pm}$ is the characteristic equation solution:

$$(\mu_i^2 + \lambda_i \mu_i + 1) = 0 \tag{9}$$

In previous work the propagation modes were characterized, as for each λ_i the roots μ_1, μ_2 of (9) satisfy $|\mu_1||\mu_2| = 1$; then two possibilities arise. If $|\mu_1| < 1 < |\mu_2|$, then we define $\mu_i^+ = \mu_1$, $\mu_i^- = \mu_2$, whereas if $|\mu_1| = |\mu_2| = 1$, the selection is done on the basis of the group velocity, which results in $\mathrm{Im}(\mu_i^+) > 0$.[30]

We denote by G the matrix $G = \mathrm{diag}(\mu_1(\lambda), \ldots, \mu_{N_{\mathrm{lay}}}(\lambda))$ and based on equation (8), it is easy to prove that equation (6) is satisfied exactly for 'forward' propagation modes by means of the relation

$$(\eta^+)^{j+1} = \mathbf{F}(\eta^+)^j \tag{10}$$

such that the F matrix named the planar DNL matrix can be given by $\mathbf{F} = VGV^{-1}$.

Then, by means of this procedure developed for the rectangular Cartesian co-ordinates,[29,30] we obtain the corresponding DNL matrix $\mathbf{F}^M = \mathbf{F}$ for the layer $j = M$:

$$(\eta^+)^{M+1} = \mathbf{F}^M(\eta^+)^M \tag{11}$$

3.2. Derivation of the DNL method in the near field

The derivation of the DNL method in the near field is obtained by means of the recursive process of calculus from the far field ($j = M$) to the near field ($j = 1$) (see Figure 3 (right)).

Substituting (11) into (5) for the layer $j = M$, and solving (5) for $(\eta^+)^M$, we obtain the DNL matrix for the layer $j = M - 1$:

$$\mathbf{F}^{M-1} = -(\mathbf{A}^M\mathbf{F}^M + \mathbf{B}^M)^{-1}\mathbf{C}^M \tag{12}$$

Repeating recursively this calculation from layer $j = M - 1$ to $j = 1$ (the layer corresponding to $r = r_{\mathrm{i}}$) we obtain the DNL matrix for layer $r = r_{\mathrm{i}}$ and the relation

$$(\eta^+)^2 = \mathbf{F}^1(\eta^+)^1 \tag{13}$$

on the artificial boundary $r = r_{\mathrm{i}}$. This relation in the near field represents a discrete non-local solution of the exterior problem governed by the Helmholtz equation. We note that the F^1 matrix contains all the information on the behaviour of the scattered wave field since the far field.

This process is numerically stable and is named 'condensation from the plane DNL matrix to the circular DNL matrix'.

We note that the solution of the exterior problem (1)–(2) is influenced by the location of the $r = r_{\mathrm{e}}$ external boundary, where is calculated the rectangular DNL condition. In previous work Bonet *et al.*[31] verified that the scattering errors along the $r = r_{\mathrm{i}}$ boundary will diminish as the circle $r = r_{\mathrm{e}}$ is placed far away from the computational domain. In this process, the CPU time increases with the exterior radius r_{e}, without increasing the RAM memory. We recall that, in general, these kinds of applications are memory bounded. Furthermore, the number of operations can be drastically reduced by means of an eigenvalue decomposition of the matrix $\mathbf{M}^{-1}\mathbf{K}$.

Such a procedure has been developed for the study of radiation and scattering water waves around a circular island.[29,31]

4. NUMERICAL RESULTS

4.1. Scattering of a plane wave from a circular island

We have computed the scattering of an incident plane wave travelling along the positive x-axis ($\theta = 0$) (by a circular island of radius r_a and depth $= 4{\cdot}0r_a$), in a normal direction to the cylinder's axis. We consider a hard boundary along the coast and the DNL boundary condition at the far boundary. With a condensation width of 8 wavelengths the numerical results are presented.

Figure 4 shows the absolute values of the analytical/numerical solution, for different values of radius $R = r_a$, $2r_a$ and $3r_a$. In this Figure, the numerical solutions represent the expected physical behaviour of the solution. Numerical solutions about this problem have been reported by Zienkiewicz *et al.*[9,10] for the relation depth $= 5{\cdot}0r_a$, and by Chen[20] and Berkhoff[12] for the relation $kr_a = 2{\cdot}0$.

4.2. Diffraction calculations for waves incident on an island located on a paraboloidal shoal

An island of circular cylindrical shape, located on a paraboloidal shoal in an infinite ocean of constant depth is attacked by small amplitude regular waves of long period and of plane incidence (see Figure 1). The wave field around the island is calculated according to diffraction theory. The bathymetry for this case is shown in Figure 1. This type of island is seemingly accepted as being representative for some real cases.[1,2,4,5]

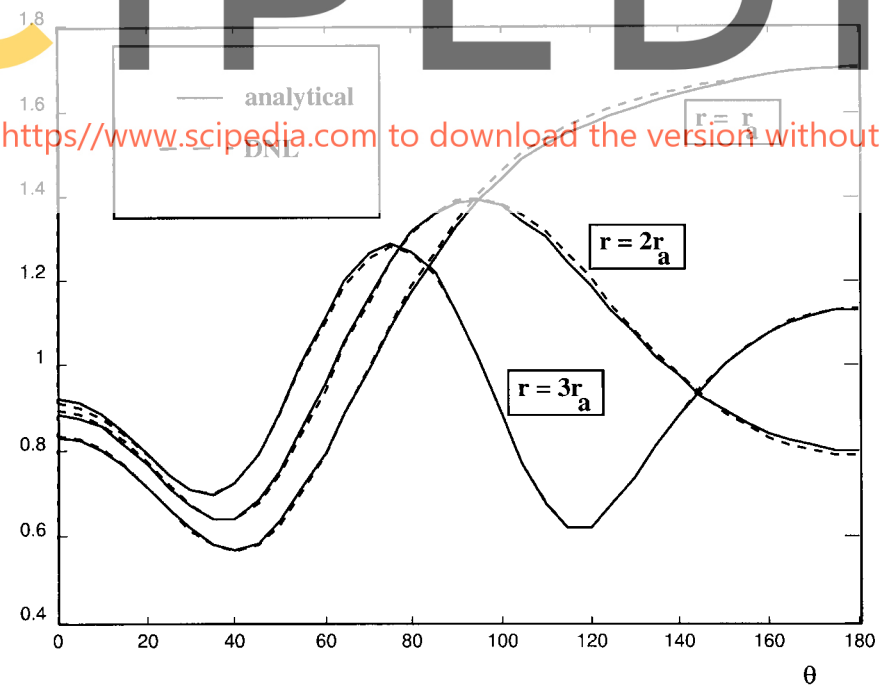

Figure 4. Scattering of a plane wave (at $\theta = 0$) from a circular island of radius r_a, $kr_a \cong 1{\cdot}23$. Absolute values of the nodal interpolation of the series solution and the Galerkin solution

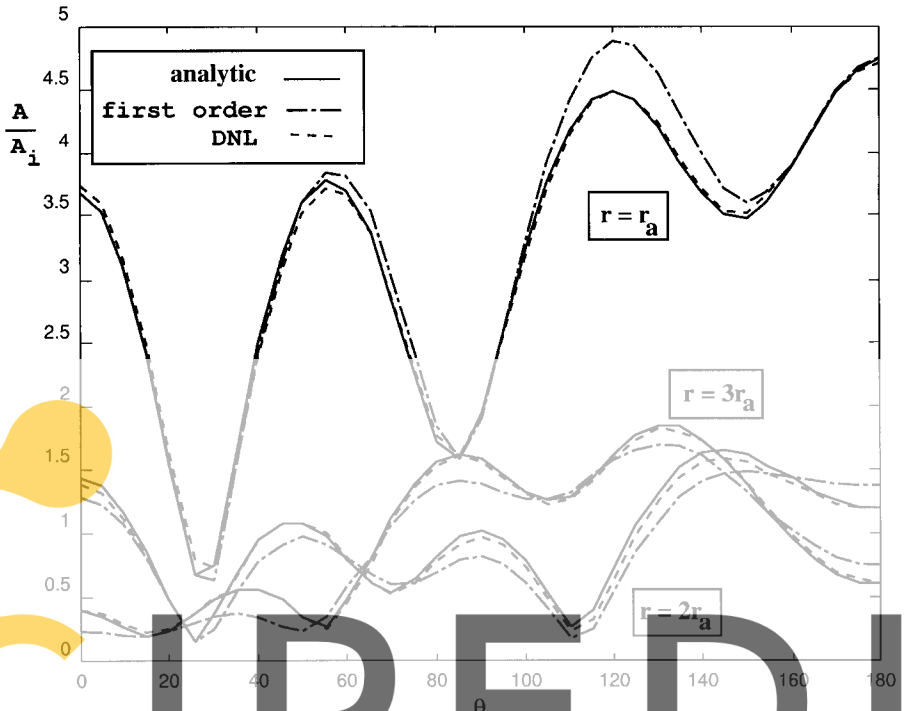

Figure 5. Relative amplitude A/A_i vs. azimuth $\theta°$

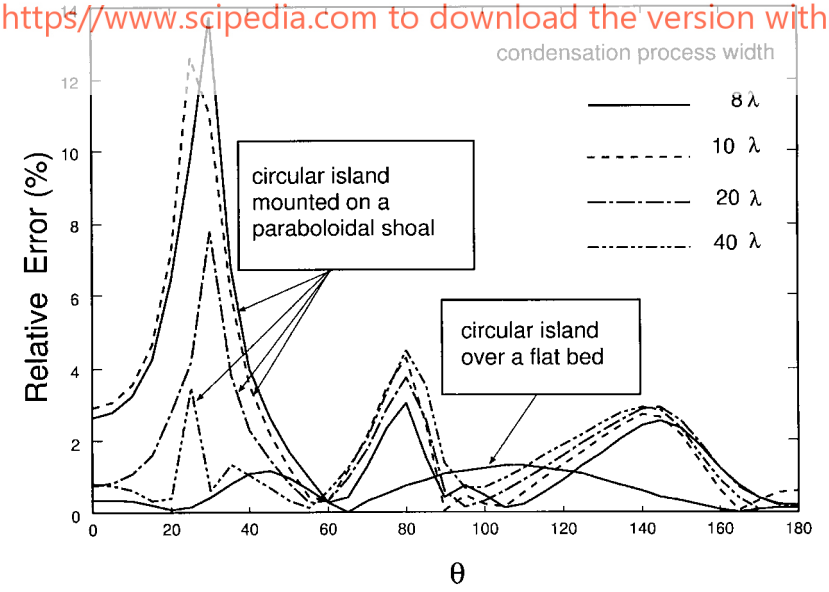

Figure 6. Relative errors at shoreline vs. azimuth $\theta°$

In the shallow water approximation the diffraction problem has an analytical solution. For this case, Homma[1] solved the infinite set of linear two-point boundary problems. Figure 5 depicts curves of relative amplitudes A/A_i at $r = r_a$, $r = 2r_a$ and $r = 3r_a$ vs. azimuth θ°. The relative amplitudes at the shoreline (with a radius of $r_a = 10$ km) correspond to the results reproduced in other papers[13,15] for a period of $T = 240$ s. This curve has the same form as the curve obtained by Zienkiewicz *et al.* for this period, but there is a discrepancy with the relative amplitudes reported by them, due to the difference in the geometrical parameters relative to the parabolic shoal. We note that, for the same period, if α increases, then the relative amplitudes at the island also increase.

The numerical solutions (Figures 4 and 5) by the finite element method and the DNL procedure were obtained when the radius $r = r_e$ is located 8λ from the artificial boundary. Figure 6 shows the corresponding relative errors (in per cent) at the island with the continuous right line. We can observe that the maximum relative errors diminish as the circle $r = r_e$ is placed far away from the computational domain. It is interesting to study how the wave at the island is delayed compared to the far field for the same value of r. In other words, the phase delay ('local phase lag') tells us how much the presence of the island plus the shoal has retarded the 'undisturbed' wave field.[2] This can be expressed at the position r as[2]

$$\Psi = \phi - kr\cos\theta \tag{14}$$

where the angle ϕ is by definition the phase lag relative to the incident waves in the far field at $\theta = \pm 90^\circ$. Figure 7 presents the phase delay Ψ vs. azimuth θ°. The numerical results are similar to results obtained by Jonsson *et al.*[2]

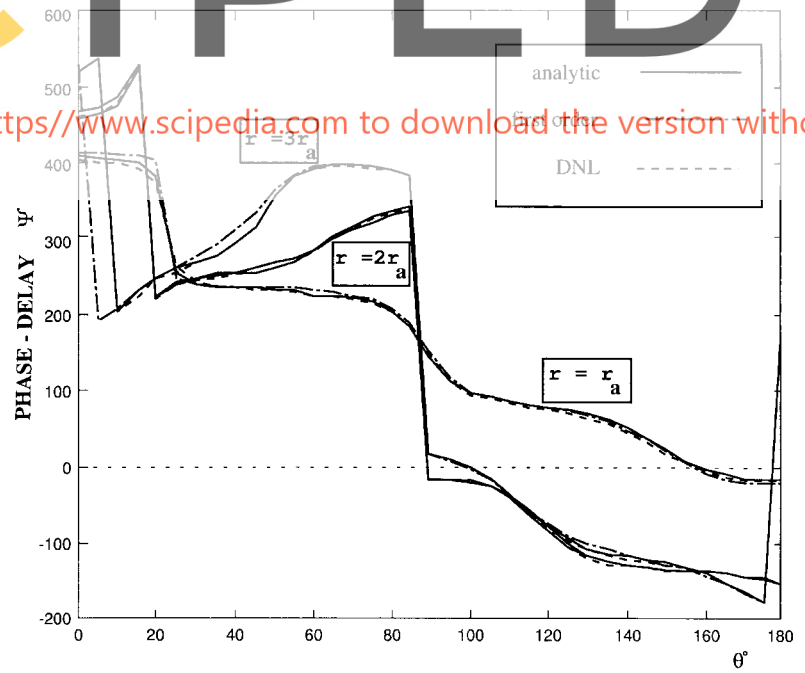

Figure 7. Phase-delay Ψ° vs. azimuth θ°. Comparison numerical vs. analytical solution based in shallow water diffraction theory

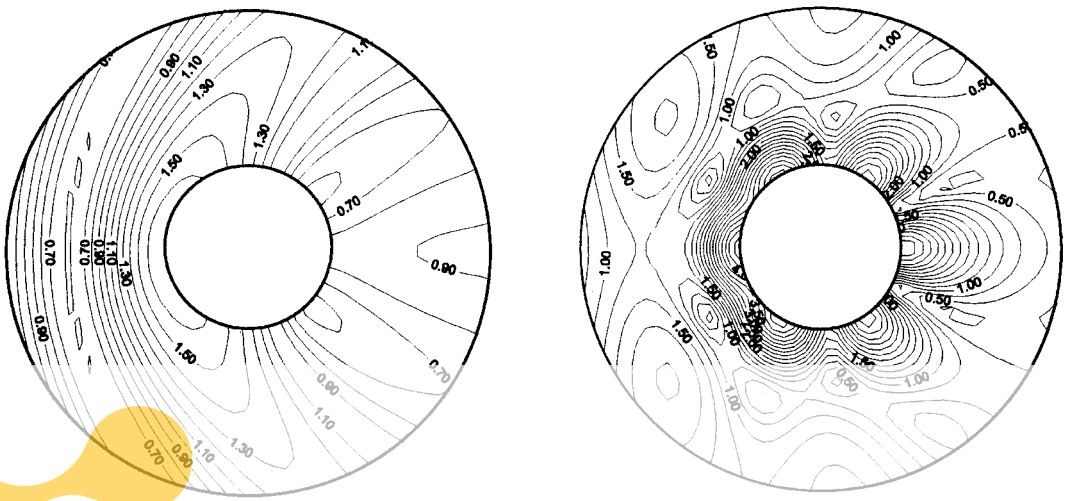

Figure 8. Scattering of a plane wave (at $\theta = 0$) from a circular island: (left) located on a constant ocean; (right) located on a paraboloidal shoal

Figure 8 shows the influence of the shoal on the scattered waves. Note that the shoal has retarded the 'undisturbed' wave field, and originates a new area of 'geometrical shadow'. In the shallow water approach, it acts as a 'waveguide', since here the phase velocity is proportional to the distance from the centre of the island.

5. CONCLUSIONS

In this paper an approach to solving long water wave propagation numerically has been shown using two diffraction problems as examples. The DNL numerical solution for long waves scattered by a circular island standing in open sea of constant depth was presented. A novel numerical solution has been developed for water wave propagation in a region of variable water depth. Employing the same condensation width as the previous case, its solution has been obtained. After comparing the results obtained with and without a shoal over the depth, we found that an island located on the paraboloidal shoal induced very strong wave amplifications near the coastline, as expected. The comparison between the numerical result employing the DNL method and the first order local condition shows the improvement of these procedures.

APPENDIX: NOMENCLATURE

$\mathcal{B}$ = circumference of radius r_i
η = water elevation
η^{s} = scattered field
η_{i} = incoming field (or incoming wave)
$\mathbf{A}_{\mathrm{i}}$ = incoming field (or incoming wave amplitude)
Δ = Laplacian operator
$k_0 = 2\pi/L_0$ wave number

r = radial polar co-ordinate
θ = angular polar co-ordinate
Ω = finite element computation domain
Ω' = outside computation domain
i = $\sqrt{(-1)}$ imaginary unit
Γ = boundary surface
h = water depth
L = wavelength
L_0 = wavelength of wave front
ω = wave angular frequency
n = outward normal on Γ
C = wave celerity
r_i = interior radius from annular region
r_e = exterior radius from annular region
T = wave period
$\dot{\phi}$ = derivate of ϕ with respect to x
$\mathbf{M}$ = mass assembled matrix
$\mathbf{K}$ = stiffness assembled matrix
$\mathbf{I}$ = identity matrix
$\mathbf{A}^j$ = matrix corresponding to $j-1$ layer
$\mathbf{B}^j$ = matrix corresponding to j layer
$\mathbf{C}^j$ = matrix corresponding to $j+1$ layer
$\mathbf{F}^j$ = DNL matrix at j layer
$\mathbf{F}$ = DNL matrix
j = layer index
n = transversal mode number
λ = wavelength
a = radius of cylinder
R = radial distance
N_{lay} = number of nodes per layer

ACKNOWLEDGEMENTS

This work has received financial support from Consejo Nacional de Investigaciones Científicas y Técnicas (CONICET, Argentina) through grant BID 802/OC-AR PID 26, and from Universidad Nacional del Litoral (Argentina). We made extensive use of software distributed by the Free Software Foundation/GNU-Project: Linux ELF-OS, Octave, Tgif from William C. Cheng, Fortran f2c compilers, and others. We also wish to thank the reviewers by their accurate comments and suggestions.

REFERENCES

1. S. Homma, 'On the behaviour of seismic sea waves around circular island', *Geophys. Mag.*, **XXI**, 199–208 (1950).
2. I. G. Jonsson, O. Skovgaard and O. Brink-Kjaer, 'Diffraction and refraction calculations for waves incident on an island', *J. Mark. Res.*, **343**, 468–496 (1976).

3. R. P. Shaw, 'Boundary integral equation methods applied to water waves', *AMD*, Vol. 11, Boundary integral equation method: Computational applications in applied mechanics, 1975, *ASME* (presented at 1975 Applied Mechanics Conference, the Rensselear Polytechnic Institute, Troy, New York, 23–25 June, 1975, T. A. Cruse and F. Rizzo (Eds.)).
4. A. C. Vastano and R. O. Reid, 'A numerical study of the tsunami response at an island', Dept. of Oceanography, Texas A & M Univ., *A & Project 471, Ref. 66-26T*, 1966, 141 pp.
5. A. C. Vastano and R. O. Reid, 'Tsunami response for islands: Verification of a numerical procedure', *J. Mar. Res.*, **25**, 129–139 (1967).
6. O. C. Zienkiewicz, 'The finite element method and boundary solution procedures as general approximation methods for field problems', World Congress on Finite Element Methods in Structural Mechanics, Bournemouth, 12–17 October 1975.
7. O. C. Zienkiewicz, D. W. Kelly and P. Bettess, 'The coupling of the finite element method and boundary solution procedures', *Int. j. numer. methods eng.*, **11**(2), 355–375 (1977).
8. O. C. Zienkiewicz, D. W. Kelly and P. Bettess, 'Marriage á la mode — or The Best of Both Worlds. Boundary integrals and finite element procedures', *Conf. on Innovative Methods of Numerical Computation*, Versailles, France, May 1977.
9. O. C. Zienkiewicz, P. Bettess and D. W. Kelly, 'The finite element method for determining fluid loading on rigid structures: two and three-dimensional formulations', in *Numerical Methods in Offshore Engineering*, O. C. Zienkiewicz, R. W. Lewis and K. G. Staff (Eds.), Wiley, 1978, Chap. 4.
10. P. Bettess and O. C. Zienkiewicz, 'Diffraction and refraction of surface waves using finite and infinite elements', *Int. j. numer. methods eng.*, **11**, 1271–1290 (1977).
11. O. C. Zienkiewicz and P. Bettess, 'Infinite elements in the study of fluid-structure interaction problems', *2nd International Symposium on Computing Methods in Applied Science and Engineering*, Versailles, France, 15–17 December 1975.
12. J. C. W. Berkhoff, 'Mathematical models for simple harmonic linear water waves, wave diffraction and refraction', Delft Hydraulic Laboratory, *Public. Nro. 163*, 1976.
13. H. S. Chen and C. C. Mei, 'Oscillations and wave forces in an offshore harbor: Applications of hybrid finite element method to water-wave scattering', Ralph M. Parsons Laboratory for Water Resources and Hydrodynamics, Mass. Inst. Tech., *Rep. No. 190*, 1974.
14. H. S. Chen and C. C. Mei, 'Oscillations and wave forces in a man-mode harbor in the open sea', presented at the *10th Naval Hydrodynamics Symposium*, June 1974.
15. H. S. Chen and C. C. Mei, 'Hybrid-element method for water waves', *Proceedings of the Modelling Techniques Conference (Modelling 1975)*, Vol. 1, San Francisco, 3–5 September 1975, pp. 63–81.
16. T.-K. Tsay and P. L.-F. Liu, 'A finite element model for wave refraction and diffraction', *Appl. Ocean Res.*, **5**, 30–37 (1983).
17. J. R. Houston, 'Combined refraction and diffraction of short waves using the finite element method', *Appl. Ocean Res.*, **3**, 163–170 (1981).
18. B. Xu, V. G. Panchang and Z. Demirbilek, 'Exterior reflections in elliptic harbor wave models', *J. Waterway Port Coastal Ocean Eng.*, **122**, 118–126 (1996).
19. R. P. Bonet, N. Nigro and M. A. Storti, 'Open boundary conditions for elliptic water wave models (CIMAF97)', La Havana, 24–27 March 1997.
20. H. S. Chen, 'Infinite elements for water wave radiation and scattering', *Int. j. numer. methods fluids*, **11**, 555–569 (1990).
21. D. Givoli and J. B. Keller, 'Non-reflecting boundary conditions for elastic waves', *Wave Motion*, **12**, 261–279 (1990).
22. D. Givoli, *Numerical Methods for Problems in Infinite Domains*, Elsevier, Amsterdam, 1992.
23. I. Harari and T. J. R. Hughes, 'Studies of domain-based formulations for computing exterior problems of acoustics', *Int. j. numer. methods eng.*, **37**, 2935–2950 (1994).
24. R. W. Thatcher, 'On the finite element method for unbounded regions', *SIAM J. Numer. Anal.*, **15**(3), 456–477 (1978).
25. R. W. Thatcher, 'The use of infinite grid refinements at singularities in the solution of Laplace's equation', *Numer. Math.*, **25**, 163–178 (1976).
26. G. Dasgupta, 'Sommerfeld's radiation condition and cloning algorithm', *ASCE-ASME Summer Conference*, Boulder, CO, 1981.

27. Ch. Song and J. P. Wolf, 'Consistent infinitesimal finite-element cell method: Three dimensional vector wave equation', *Int. j. numer. methods eng.*, **39**, 2189–2208 (1996).
28. J. P. Wolf and Ch. Song, *Finite Element Modelling of Unbounded Media*, Wiley, 1996, 331 pp.
29. R. P. Bonet, N. Nigro, M. A. Storti and S. R. Idelsohn, 'Non-local absorbing discrete boundary condition (DNL) in finite difference for water waves elliptic models' (in Spanish; submitted to RIMNE, 1997).
30. R. P. Bonet, N. Nigro, M. A. Storti and S. R. Idelsohn, 'Non-local absorbing discrete boundary condition (DNL) in finite elements for water waves elliptic models' (in Spanish; submitted to RIMNE, 1997).
31. R. P. Bonet, N. Nigro, M. A. Storti and S. R. Idelsohn, 'Discrete non-local absorbing discrete boundary condition for exterior problems governed by Helmholtz equation' (submitted for publication to *Int. j. numer. methods fluids*, 1997).
32. M. A. Storti, J. D.'Elía and S. R. Idelsohn, 'Algebraic discrete non-local (DNL) for the ship wave resistance problem' (submitted for publication to *J. Comput. Phys.*, 1997).
33. R. P. Shaw, 'Transient scattering by a circular island', *J. Sound Vib.*, **42**(3), 295–304, (1975).

